Supplementary Material for "Large Magnetodielectric Coupling in Layered Perovskite Eu_2TiO_4"

Yang Zhang,[1] Yudai Hasegawa,[1] Shingo Kitano,[1] Lihong Liu,[3] Tohru S. Suzuki,[3] Wei Yi,[1] Hirofumi Akamatsu,[2] and Koji Fujita[1*]

[1]*Department of Material Chemistry, Graduate School of Engineering, Kyoto University, Katsura Nishikyo-ku, Kyoto 615-8510, Japan*
[2]*Department of Applied Chemistry, School of Engineering, Kyushu University, Motooka, Fukuoka 812-0053, Japan*
[3]*Optical Ceramics Group, Research Center for Electronic and Optical Materials, National Institute for Materials Science, Tsukuba, Ibaraki, 305-0047 Japan*
E-mail: fujita.koji.5w@kyoto-u.ac.jp

1. Mössbauer spectroscopy

To evaluate the valence state of europium ions and the local environment around Eu^{2+} ions, ^{151}Eu Mössbauer effect measurements were performed at room temperature using a standard transmission geometry. A $^{151}Sm_2O_3$ source with 1.85 GBq activity provided the 21.5 keV γ-ray emission, and the velocity calibration was done with the magnetic hyperfine spectrum of α-Fe foil obtained using ^{57}Co doped Rh as a 14.4 keV g-ray source. The Mössbauer spectrum of EuF_3 was measured as a standard of Doppler velocity.

Figure S1 shows the room-temperature ^{151}Eu Mössbauer spectrum of $n = 1$ RP-type Eu_2TiO_4. Two absorption peaks are observed around 11.9(1) and 0.5(1) mm/s, assigned to Eu^{2+} and Eu^{3+}, respectively. From the area ratio of the two absorption peaks, the fraction of Eu^{2+} relative to the total europium ions was estimated to be about 0.98(1). Since the effective Debye temperature of Eu^{2+} is usually lower than that of Eu^{3+} (*e.g.* 195 K for Eu^{2+} and 220 K for Eu^{3+} in $EuPd_3S_4$ [1]), it is expected that the real fraction of Eu^{2+} is higher than 98%. Note that the fraction of Eu^{2+} in the present sample is relatively larger than that in Eu_2TiO_4 as reported previously (~96%) [2].

The isomer shifts (δ = –11.9 mm/s) for Eu_2TiO_4 at room temperature is slightly larger than that of $EuTiO_3$ (δ = –12.5 mm/s) [3], indicating a reduced coordination number for Eu^{2+} (CN = 9) than $EuTiO_3$ (CN = 12).

At 300 K, the Mössbauer spectrum can be interpreted in terms of pure quadrupole effects with quadrupole interactions $eV_{zz}Q_g$ = –6.1 mm/s. Since the Eu^{2+} site has fourfold symmetry, the asymmetry parameter η is regarded as zero. The fitting results for the Mössbauer data are summarized in Table S1.

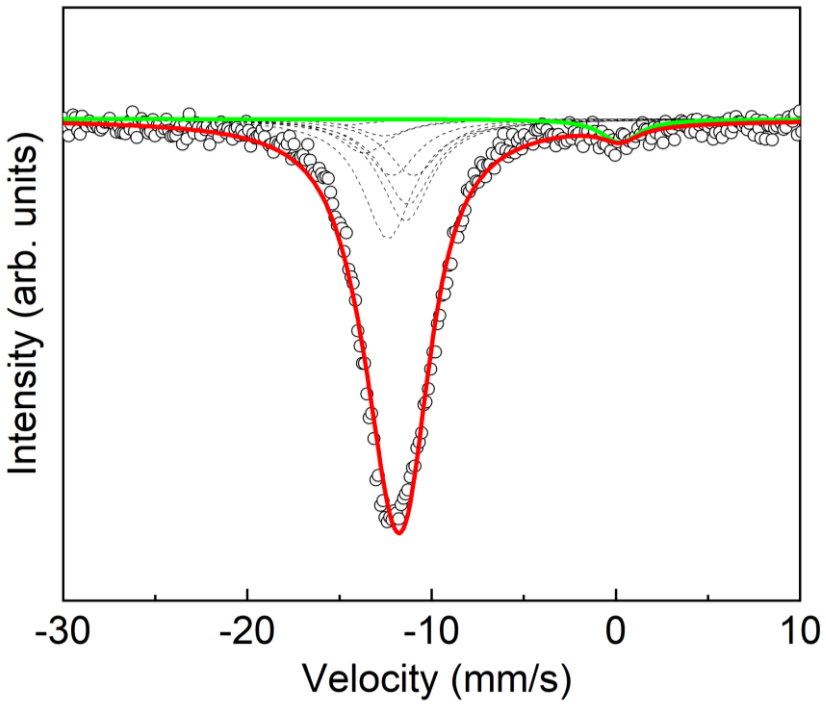

Fig. S1 Mössbauer spectrum of n = 1 RP-type Eu_2TiO_4 at room temperature. The black circles and red solid lines represent the experimental data and calculated curve, respectively. The green solid line shows the contribution from Eu^{3+} absorption.

Table S1 The fitting parameters for Mössbauer spectrum of n = 1 RP-type Eu_2TiO_4

	A_{Eu}^{2+} / A_{Eu}^{3+}	δ (mm/s)	$eV_{zz}Q_g$ (mm/s)
Eu_2TiO_4	0.98	−11.9(1)	–6.1(4)
Eu_2TiO_4 [2]	0.96	−11.8	–6.6
$EuTiO_3$ [3]	0.96	−12.5(1)	0
$EuZrO_3$ [4]	0.94	−12.9(1)	–10.20(37)

Table S2 Structural parameters of n = 1 RP-type Eu_2TiO_4 at 300 K obtained from refinement with an $I4/mmm$ model against the SXRD data

	Site	x	y	z	Occ.	U
Eu1	4e	0	0	0.35414(2)	1	0.0050(5)
Ti1	2a	0.5	0.5	0.5	1	0.004(21)
O1	4c	0.5	0	0.5	1	0.008(10)
O2	4e	0	0	0.15971(23)	1	0.0050(6)

2. Molecular-field approximation

In Eu^{2+}-containing oxides with perovskite-type structure, the magnetic structure is predominantly determined by the nearest-neighbors (NN) and next-nearest-neighbor (NNN) exchange interactions between Eu^{2+} ions. In the case of cubic systems such as $EuTiO_3$, these exchange interactions are characterized by the exchange constants J_1 and J_2, respectively. In the layered perovskite oxide, Eu_2TiO_4, however, there exist three types of NN of Eu^{2+} (J_{11}, J_{12}, J_{13}) [see the inset of Fig. S2(a)] and two types of NNN Eu^{2+} (J_{21}, J_{22}) [see the inset of Fig. S2(b)]. We used the exchange interaction parameters obtained with the previous first-principles calculations [4]: J_{11}/k_B = 0.2 K, J_{12}/k_B = 0.08 K and J_{13}/k_B = 0.0 K for NN interactions, J_{21}/k_B = 0.08 K and J_{22}/k_B = 0.04 K for NNN interactions, where k_B is the Boltzmann constant. The calculation is done by the custom ruby code with internal molecular field components along the in-plane (x) and out-of-plane (z) directions:

$$H_x = -(4J_{11} + 4J_{12} + J_{13} + 4J_{21} + 4J_{22}) \times S_x$$

$$H_z(z, h) = -(4J_{11} + 4J_{12} + J_{13} + 4J_{21} + 4J_{22}) \times S_z - g \cdot \mu_B \cdot h$$

The total effective field is:

$$\left|H_{eff}\right| = \sqrt{H_x^2 + H_z^2},$$

where x and z are the spin components, g is the Landé g-factor, μ_B is the Bohr magneton, and h is the external magnetic field. These equations were implemented using a self-consistent iterative approach to compute the average magnetization $\langle S_z \rangle$ and the nearest-neighbor spin correlation $\langle S_i \cdot S_j \rangle$ as a function of temperature and magnetic field.

In the molecular-field calculation, $\langle S_i \cdot S_j \rangle$ obtained as the products of $\langle S \rangle$ on two sublattices in different magnetic fields are shown in Fig. S2(a). To further analyze the impact of a magnetic field on the dielectric properties, we calculated the change in spin pair correlation: $\Delta\langle S_i \cdot S_j \rangle = \langle S_i \cdot S_j \rangle_H - \langle S_i \cdot S_j \rangle_0$ The T_C determined from the peak position of $\Delta\langle S_i \cdot S_j \rangle$ is approximately 9.5 K [as shown in Fig. S2(b)], in good agreement with our experimental result.

Table S3 Eu-Eu coordinates, distance, and direction in Eu_2TiO_4.

NN	NNN	Coordinates	Distance(Å)	Direction
J_{11}		4	3.79123(1)	<11√2>
J_{12}		4	3.88619(2)	<100>
J_{13}		1	3.65819(5)	<001>
	J_{21}	4	5.49590(4)	<110>
	J_{22}	4	5.33711(4)	<101>

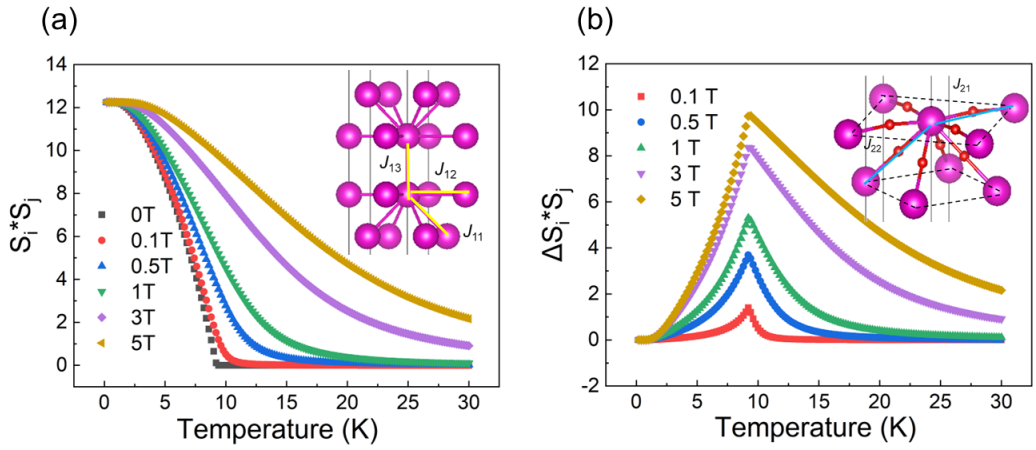

Fig. S2 (a) Spin correlation function $<S_i \cdot S_j>$ for Eu_2TiO_4 calculated using a molecular-field approximation at H = 0, 0.1, 0.5, 1, 3, and 5 T. (b) Temperature dependence of $\Delta<S_i \cdot S_j>$ obtained by subtracting $<S_i \cdot S_j>$ data at H = 0.1, 0.5, 1, 3, and 5 T data from those at H = 0 T. The inserts show the NN interactions J_{1m} (m = 1, 2, 3) and NNN interactions J_{2n} (n = 1, 2) in Eu_2TiO_4

3. Phonon band structure and phonon model

Based on the crystal symmetry, there are 18 types of optical phonon modes in *I*4/*mmm* Eu_2TiO_4. Among these, 7 infrared transverse optical (TO) modes mainly influence the dielectric properties. Our first-principles calculations reveal that the E_u (TO1) mode has the lowest frequency (see table S4), making it the dominant contributor to the dielectric properties. In this mode, Ti^{4+} and Eu^{2+} ions vibrate against the O^{2-} octahedra within the *a*-*b* plane (see the inset of Fig. 2 in the main text), resembling the T_{1u} mode in $EuTiO_3$ [5].

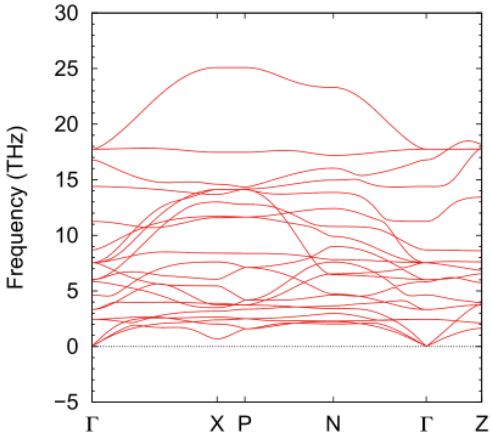

Fig. S3 (a) Phonon band structure of Eu_2TiO_4. The symmetry points are based on the $\sqrt{2} \times \sqrt{2} \times 2$ supercell.

Table S4 Phonon frequencies (cm^{-1}) and mode assignments at Γ point in Eu_2TiO_4

Irrep	A_{2u}**(TO1)**	A_{2u}**(TO2)**	A_{2u}**(TO3)**	E_u**(TO1)**	E_u**(TO2)**	E_u**(TO3)**	E_u**(TO4)**
Freq (cm^{-1})	194	375	489	111	200	251	592

According to previous investigations of bulk $EuTiO_3$ [5], a strong coupling between Eu spins and dielectric properties was realized through a modified T_{1u} phonon mode. This was confirmed by an abrupt change in permittivity in different magnetic fields. In Eu_2TiO_4, this coupling is associated with the E_u(TO1) mode. The magnitude of the change in phonon frequency (ω_0) with an applied magnetic field can be estimated from that of the permittivity. We speculate that the hybridization between Eu-4f/Ti-3d orbitals varies depending on the configuration of the Eu spins, which then modifies the E_u(TO1) mode frequency. As shown in Fig. 3(b) of the main text, the permittivity increases monotonically with the applied magnetic field and saturates at 3 T, reaching an increasement of approximately 22%. According to the Lyddane-Sachs-Teller (LST) relation, this increase in permittivity corresponds to a softening of the E_u(TO1) mode, with an estimated decrease in ω_0 by 11%. The calculation follows the formula:

$$\varepsilon(\omega) = \varepsilon_1(\omega) - i\varepsilon_2(\omega) = \varepsilon_\infty + \frac{4\pi N e^{*2}/\mu}{(\omega_0^2 - \omega^2) + i\Gamma\omega}$$

where N is the number of unit cells per volume, e^* is the effective charge of ions, μ is the effective mass of ions, ω_0 is the phonon frequency, and Γ is the scattering rate of the phonon.

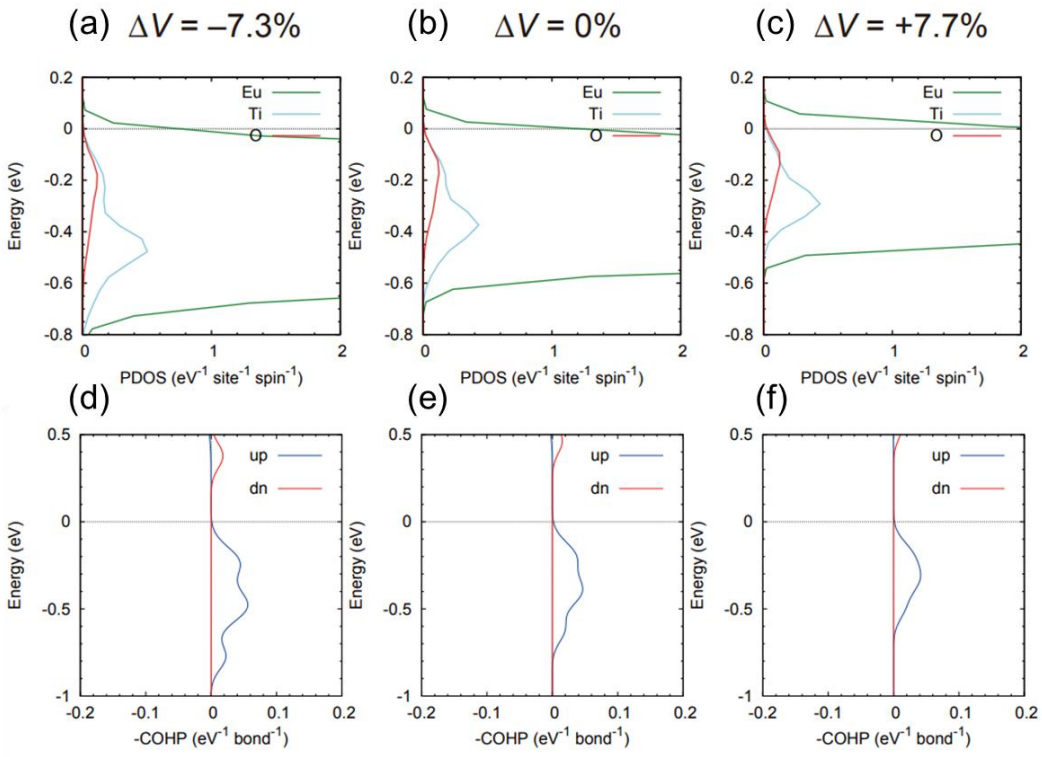

Fig. S4 Upper panel: Magnified view of the up-spin component of the PDOS in the energy region near the Eu 4f band of Eu_2TiO_4 at (a) $\Delta V = -7.3\%$, (b) 0%, and (c) +7.7%. Lower panel: Negative crystal orbital Hamilton populations (−COHP) for Eu-Ti interactions near the Fermi level at (d) $\Delta V = -7.3\%$, (e) 0%, and (f) +7.7%. The highest occupied state (Fermi level) is set to 0 eV.

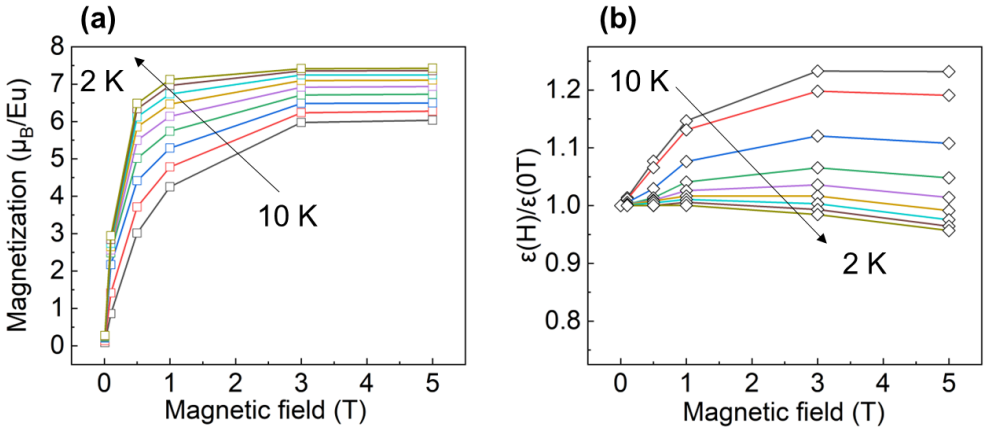

Fig. S5 (a), (b) Magnetic field dependence of (a) magnetization and (b) dielectric permittivity ratio [$(\varepsilon(H)/\varepsilon(0\text{T})$ at 1 MHz], for various temperatures (2, 3, 4, 5, 6, 7, 8, 9, and 10 K) in the range 0 T ≤ H ≤ 5 T.

Reference:

[1] M. Wakeshima *et al.*, J. Solid State Chem. **157**, 117 (2001).

[2] Chia-Ling Chen and F. De S. Barros, Phys. Lett. A **38**, 427 (1972).

[3] C.-L. Chien, S. DeBenedetti, and F. D. S. Barros, Phys. Rev. B **10**, 3913 (1974).

[4] S. Li *et al.*, J. Mater. Chem. C **11**, 8383 (2023).

[5] T. Katsufuji and H. Takagi, Phys. Rev. B **64**, 054415 (2001).